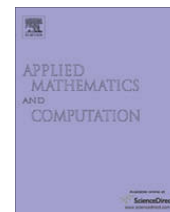




Contents lists available at ScienceDirect

## Applied Mathematics and Computation

journal homepage: [www.elsevier.com/locate/amc](http://www.elsevier.com/locate/amc)

## On the non-degeneracy property of the longest-edge trisection of triangles

Ángel Plaza<sup>a,\*</sup>, Sergio Falcón<sup>a</sup>, José P. Suárez<sup>b</sup><sup>a</sup>Department of Mathematics, University of Las Palmas de Gran Canaria, Spain<sup>b</sup>Department of Cartography and Graphic Engineering, University of Las Palmas de Gran Canaria, Spain

## ARTICLE INFO

## Keywords:

Triangle subdivision  
Trisection  
Finite element method  
Mesh quality

## ABSTRACT

The longest-edge (LE) trisection of a triangle  $t$  is obtained by joining the two equally spaced points of the longest-edge of  $t$  with the opposite vertex. In this paper we prove that for any given triangle  $t$  with smallest interior angle  $\tau > 0$ , if the minimum interior angle of the three triangles obtained by the LE-trisection of  $t$  into three new triangles is denoted by  $\tau_1$ , then  $\tau_1 \geq \tau/c_1$ , where  $c_1 = \frac{\pi/3}{\arctan(\sqrt{3/5})} \approx 3.1403$ . Moreover, we show empirical evidence on the non-degeneracy property of the triangular meshes obtained by iterative application of the LE-trisection of triangles. If  $\tau_n$  denotes the minimum angle of the triangles obtained after  $n$  iterative applications of the LE-trisection, then  $\tau_n > \tau/c$  where  $c$  is a positive constant independent of  $n$ . An experimental estimate of  $c \approx 6.7052025350$  is provided.

© 2010 Elsevier Inc. All rights reserved.

## 1. Introduction

It is well known that numerical grid generation and the ability to control automatically and adaptively discretization in the numerical solution of partial differential equation is critical to the reliable application of numerical analysis techniques, specially by means of adaptive finite-element methods and multigrid algorithms [5–7,19]. In this context, non-degeneracy of the elements, conformity of the new grid and smoothness of the refinement are desirable features of the local refinement algorithms [4,11].

The algorithms based on the longest-edge bisection of triangles were developed to deal with this specific question [13,14]. These algorithms guarantee the construction of good-quality irregular and nested triangulation. This is due firstly to the boundedness condition on the small angles of the triangles so generated, and secondly to the natural refinement propagation strategy outside the target refinement area. The simplest longest-edge partition of a triangle is the longest-edge bisection. For a given triangle  $t = \triangle RST$ , and by iteratively application of longest-edge bisection to the triangle and its descendants, an infinite family of triangles may be obtained, say this family of triangles  $\mathcal{F}(R, S, T)$ . It has been proved that if  $\tau$  is the smallest interior angle of the initial triangle  $t = \triangle RST$  and  $\tau_n$  is any interior angle of any triangle  $\Delta \in \mathcal{F}$ , then  $\tau_n \geq \tau/2$  [15]. In addition, this family so obtained falls into finitely many similarity classes [17,18], and also it has been obtained sharp estimated for the longest  $j$ th generation edge [1].

It should be mentioned that there are two situations with bisection methods: techniques producing conforming (no hanging nodes) triangulations, and those which yield sometimes such hanging nodes. For example, if in a given triangulation, all the simplices are bisected simultaneously, so-called hanging nodes may appear (see Fig. 1).

The appearance of hanging nodes is a certain disadvantage especially if we want to use conforming finite-element discretizations over such partitions. Local refinement of non-conforming simplex elements by continued longest-edge subdivision may be considered in order to ensure conformity. The extent of the subsidiary-induced refinement due to the conformity is

\* Corresponding author.

E-mail address: [aplaza@dmate.ulpgc.es](mailto:aplaza@dmate.ulpgc.es) (Á. Plaza).

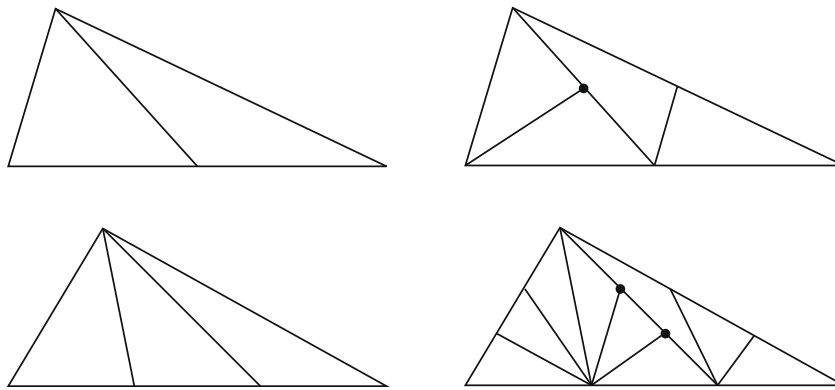


Fig. 1. Hanging nodes may appear at bisecting (or) trisecting all the triangles in a given triangulation.

an issue of practical concern since it has been noted that refinement of a single cell can propagate LE subdivisions to the boundary [16].

Several local and global algorithms based on bisection have been proposed in literature [8,10,13,14]. In the context of local refinement algorithms based on bisection of the edges an alternative to the longest-edge based algorithms is the red-green approach both in 2D and in 3D [2,3]. In 2D, the conformity of the mesh is assured by joining the hanging nodes with the opposite vertex. This partition of the non-conforming triangles is not by the longest-edge in general. In this strategy the refinement does not extent by conformity.

In this paper we first introduce an extension of the LE-bisection, also based on equally division of the longest-edge of the triangle, but now in three parts. Then, following a similar argument to reference [15], we prove that, for a given initial triangle  $t$  with smallest interior angle  $\tau > 0$ , the LE-trisection of  $t$  produces three new triangles  $t_i, i = 1, 2, 3$  such that any interior angle of  $t_i, \tau_1$  verifies  $\tau_1 \geq \tau/c_1$ , where  $c_1 = \frac{\pi/3}{\arctan(\sqrt{3/5})} \approx 3.1403$ .

Finally, empirical evidence is given of the non-degeneracy of the (non-conforming) meshes or partitions obtained by iterative application of LE-trisection. In fact, by means of a Monte Carlo computational experiment is shown that if  $\tau$  is the minimum interior angle of the initial triangle, and  $\tau_n$ , the minimum interior angle after  $n$  levels of LE-trisection, then  $\tau_n \geq \tau/6.7052025350$ , independently on the value of  $n$ .

## 2. The longest-edge trisection: Definition, notations and properties

**Definition 1.** The longest-edge bisection of a triangle  $t$  is obtained by joining the midpoint of the longest-edge of  $t$  with the opposite vertex.

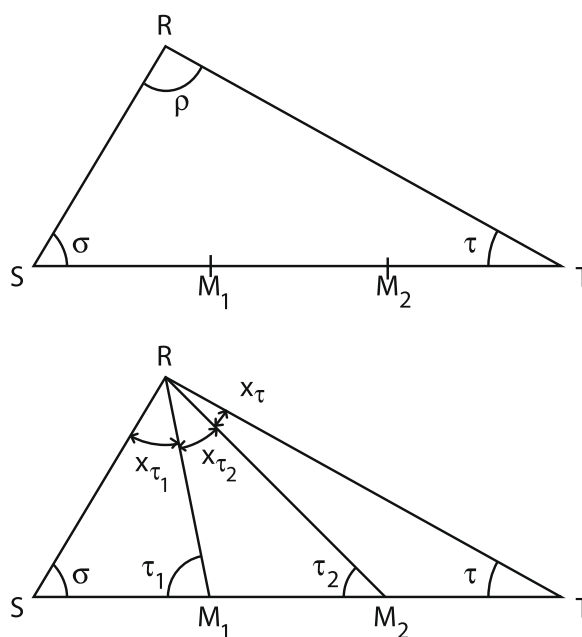


Fig. 2. Longest-edge trisection of triangle ARST.

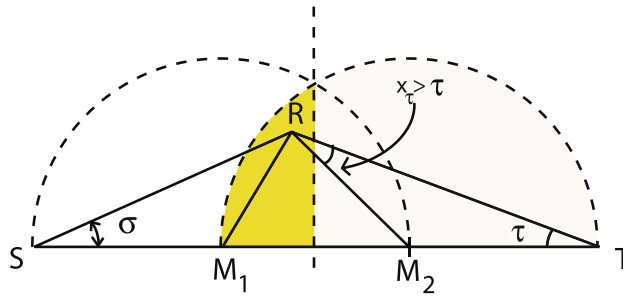


Fig. 3. Shaded area for the apex R in which  $x_\tau \geq \tau$ .

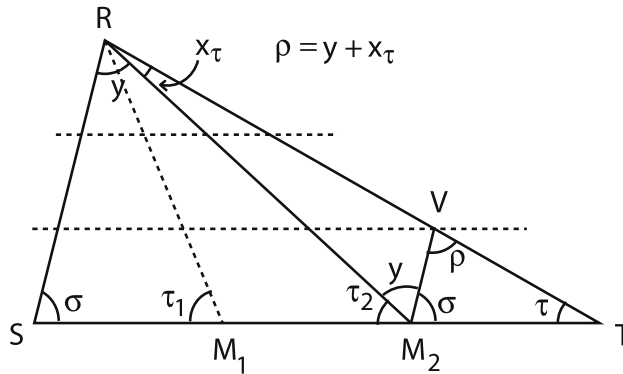


Fig. 4. LE-trisection of an isosceles triangle  $\triangle RST$  when  $|TR| = |TS|$ .

**Definition 2.** The longest-edge trisection of a triangle  $t$  is obtained by joining the two equally spaced points of the longest-edge of  $t$ , say  $M_1$  and  $M_2$ , with the opposite vertex.

Fig. 2 shows the longest-edge trisection of triangle  $\triangle RST$  with longest-edge  $ST$ .  $M_1 = S + \frac{1}{3}\overrightarrow{ST} = \frac{2S+T}{3}$  and  $M_2 = S + \frac{2}{3}\overrightarrow{ST} = \frac{S+2T}{3}$  are two equally spaced points in the longest-edge  $ST$ . Note that the angles of triangle  $\triangle RST$  are  $\tau \leq \frac{\pi}{3} \leq \sigma \leq \rho$ . The three angles in which largest angle  $\rho$  is divided will be denoted here by  $x_{\tau_1}, x_{\tau_2}$ , and  $x_\tau$  by referring to the other angle in the respective subtriangle, so  $\rho = x_{\tau_1} + x_{\tau_2} + x_\tau$ , and since  $\tau \leq \sigma$  then  $x_{\tau_1} \geq x_\tau$  and  $x_{\tau_2} \geq x_\tau$ . Note that in some cases  $x_\tau \geq \tau$  (see Fig. 3).

In which follows we consider a generic triangle  $\triangle RST$  with angles  $\tau \leq \sigma \leq \rho$ . After the LE-trisection of  $\triangle RST$ , largest angle  $\rho$  is divided in three angles  $x_{\tau_1} \geq x_\tau$  and  $x_{\tau_2} \geq x_\tau$  as in Fig. 1.

We consider first the case of an isosceles triangle with smallest angle  $\tau \leq \frac{\pi}{3}$  and two longest-edges, and also two greatest angles  $\rho = \sigma = \frac{\pi}{2} - \frac{\tau}{2}$ .

**Lemma 1.** Let  $\tau \leq \pi/3$  and  $\rho = \sigma = \pi/2 - \tau/2$ . Then the minimum interior angle of the three triangles obtained by the LE-trisection of  $t$  into three new triangles, angle  $x_\tau$  in Fig. 4, satisfies

$$\tan x_\tau = \frac{\sin \tau}{3 - \cos \tau} \geq \tan \tau/3.1403. \tag{1}$$

**Proof.** Let  $V$  be the point in edge  $RT$  such that  $M_2V$  is parallel to  $SR$ , that is  $V = \frac{2T+R}{3}$ . The law of sines in  $\triangle RM_2V$  and  $\triangle RST$  yields (see Fig. 4)

$$\frac{\sin x_\tau}{|M_2V|} = \frac{\sin y}{|VR|} \Rightarrow \frac{\sin x_\tau}{\sin y} = \frac{|M_2V|}{|VR|} = \frac{|M_2V|}{2|TV|} = \frac{\sin \tau}{2 \sin(\pi/2 - \tau/2)}.$$

So,  $\sin x_\tau \sin(\pi/2 - \tau/2) = \frac{1}{2} \sin \tau \sin y$ , and since  $y = x_{\tau_1} + x_{\tau_2} = \pi/2 - \tau/2 - x_\tau$ , we obtain

$$\sin x_\tau \cos(\tau/2) = \frac{1}{2} \sin \tau \cos(\tau/2 + x_\tau).$$

Simplifying, we get

$$\sin x_\tau \cos(\tau/2) = \sin(\tau/2) \cos(\tau/2) [\cos(\tau/2) \cos x_\tau - \sin(\tau/2) \sin x_\tau]$$

$$\sin x_\tau = \frac{1}{2} \sin \tau \cos x_\tau - \sin^2(\tau/2) \sin x_\tau$$

$$\tan x_\tau = \frac{1}{2} \sin \tau - \frac{1 - \cos \tau}{2} \tan x_\tau$$

$$\tan x_\tau = \frac{\sin \tau}{3 - \cos \tau}.$$

Note that Eq. (1) implies that  $x_\tau$  is a increasing function of the argument  $\tau$  as can be immediately proved by the derivative, and its second derivative is negative for  $\tau \in (0, \pi/3)$ . Therefore, since  $x_{\pi/3} = \arctan \frac{\sin(\pi/3)}{3 - \cos(\pi/3)} = \arctan \frac{\sqrt{3}}{5}$ , then the values of  $x_\tau$  are greater or equal than those on the secant line  $y = \frac{\arctan \frac{\sqrt{3}}{5}}{\pi/3} x \approx \frac{x}{3.1403}$  (see Fig. 5). This proves Lemma 1.  $\square$

Now, we consider fixed in a triangle the longest-edge, say  $ST$  and the smallest angle  $\tau$ , and study again the minimum angle  $x$  generated by the LE-trisection of the triangle, but in function of the second largest angle  $\sigma$ . So  $x = x_\sigma = x(\sigma)$ . Clearly,  $\sigma$  changes from  $\sigma_{\min} = \tau$  to  $\sigma_{\max} = \pi/2 - \tau/2$ , when  $\triangle RST$  becomes an isosceles triangle (see Fig. 6) in which the angles of the initial triangle are  $\rho \geq \sigma \geq \tau$ .

Note that for the case  $\sigma_{\min} = \tau$ , the largest angle of triangle  $\triangle RST$  is  $\rho = \pi - 2\tau$ . Also triangle  $\triangle M_1M_2R$  in Fig. 4 is isosceles with angles at  $M_1$  and  $M_2$  both equal to  $\tau_2 = \arctan(3 \tan \tau) < \pi/2$ , so angle at  $R$  in triangle  $\triangle M_1M_2R$  is equal to  $\pi - 2 \arctan(3 \tan \tau)$ . Therefore, angle  $x(\sigma_{\min}) = \arctan(3 \tan \tau) - \tau$ .

Clearly,  $x = x(\sigma)$  is a decreasing function of  $\sigma$  in the region  $\sigma_{\min} \leq \sigma \leq \sigma_{\max}$ , whose range of values are

$$x_\tau = x(\sigma_{\max}) \leq x(\sigma) \leq x(\sigma_{\min}) = \arctan(3 \tan \tau) - \tau.$$

For the value of  $x(\sigma_{\max})$ , we can use the result of Lemma 1, taking into account that for the case of an isosceles triangle with minimum angle  $\tau$ , and two equal greater angles, then  $\sigma = \pi/2 - \tau/2$ , so Eq. (1) reads now as

$$\tan x_\sigma = \frac{\tan \sigma}{1 + \tan^2 \sigma}.$$

Notice also that when  $\rho = \frac{2\pi}{3}$  and  $\tau = \frac{\pi}{6} = \sigma$ , then  $x(\sigma) = \arctan(3 \tan \tau) - \tau = \frac{\pi}{6}$ . Finally, it is evident by elementary trigonometry from Fig. 7 that

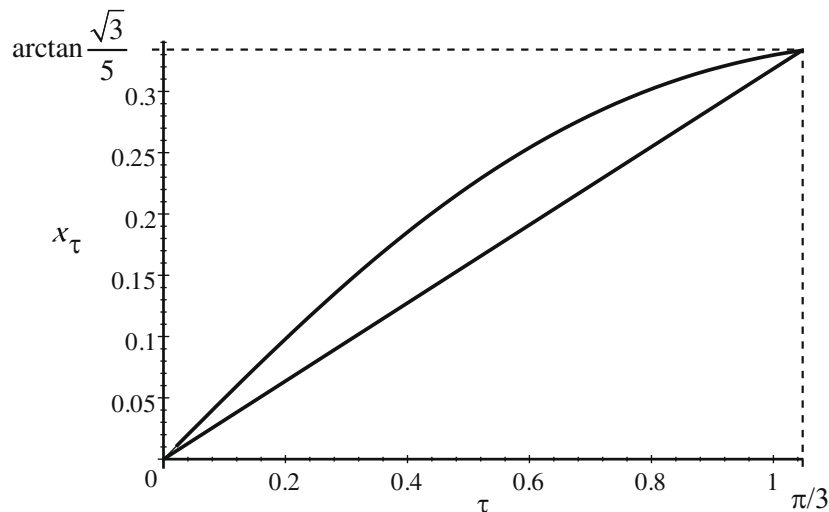


Fig. 5. Function  $x_\tau = x(\tau)$  for  $\tau \in [0, \pi/3]$ .

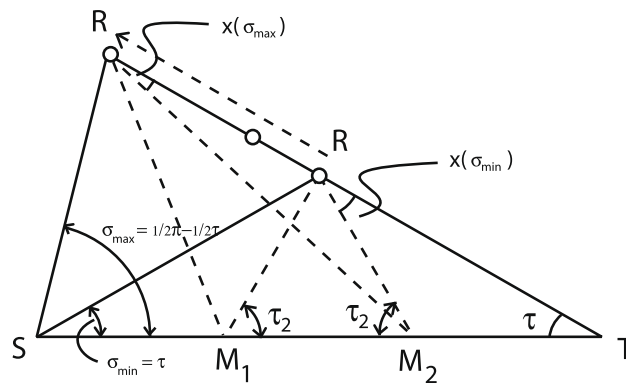


Fig. 6. Various values of the angle  $x = x(\sigma)$ .

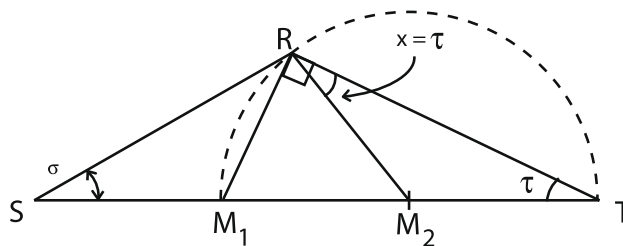


Fig. 7. Situation in which  $x(\sigma) = \tau$ .

$$x \geq \tau \iff \tau \leq \sigma \leq \arccos \frac{1 + 2 \sin^2 \tau}{\sqrt{1 + 8 \sin^2 \tau}}. \tag{2}$$

And this proves the following theorem:

**Theorem 1.** Let the smallest interior angle of  $t = \Delta RST$  be  $\lambda$ , and let  $0 < x_\lambda < \pi/6$  be the solution of

$$\tan x_\lambda = \frac{\sin \lambda}{3 - \cos \lambda}. \tag{3}$$

If  $t_i$  is a triangle obtained by the LE-trisection of  $t$ , and  $\tau_1$  is an interior angle of  $t_i$ , then  $\tau_1 \geq x_\lambda$ .

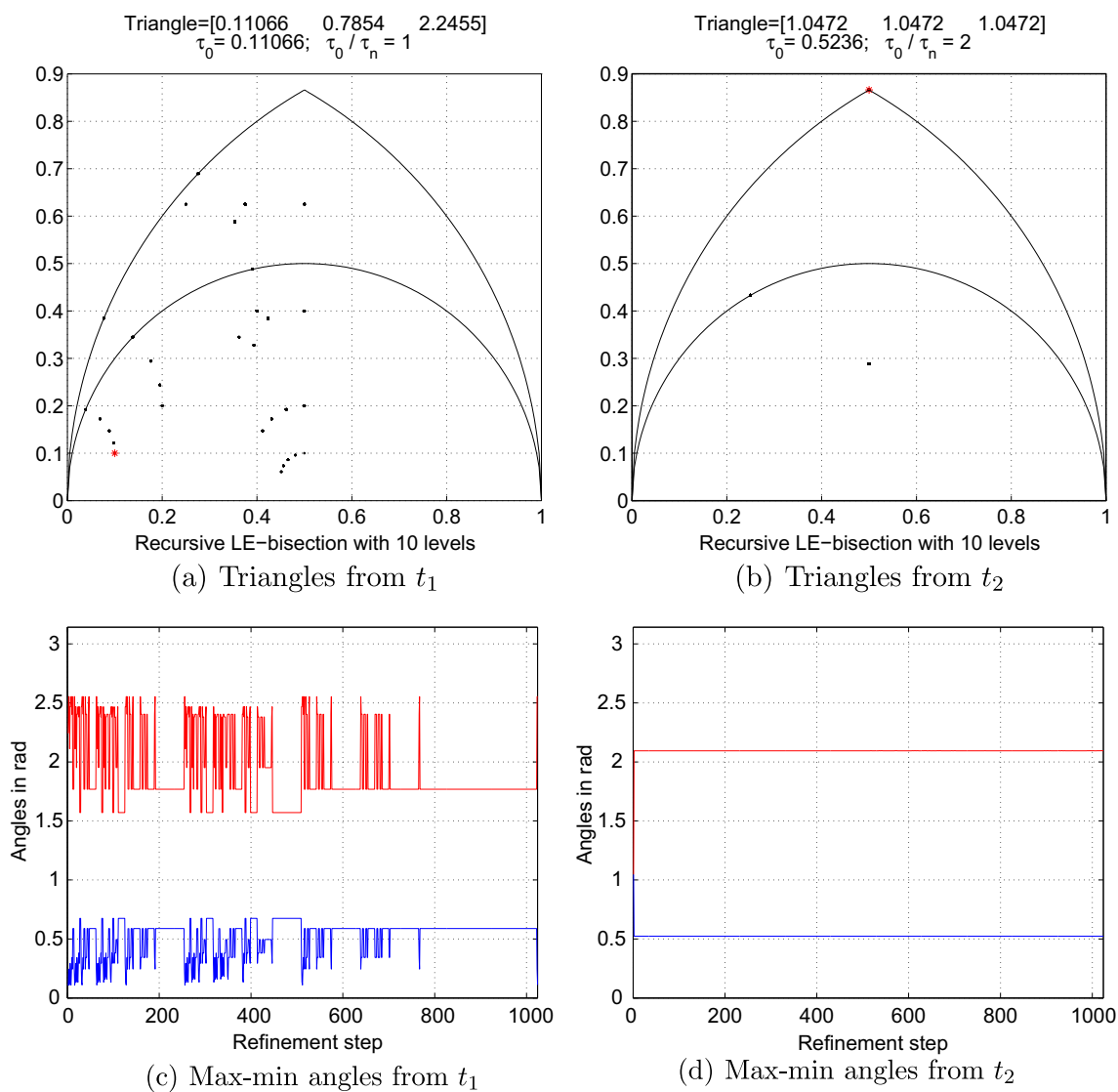


Fig. 8. Evolution of the triangles by the 2-LE partition and max-min angle evolution.

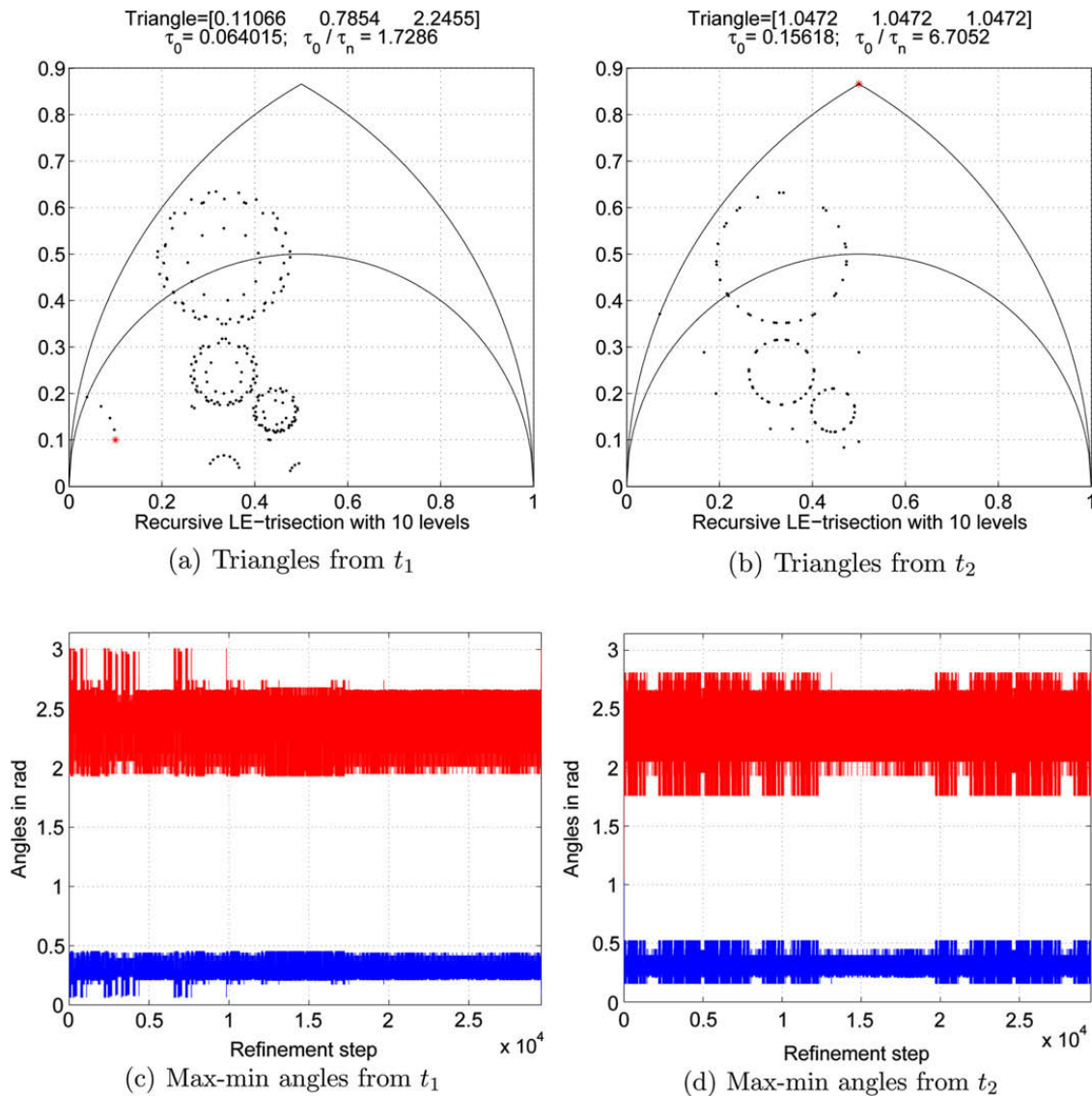


Fig. 9. Evolution of the triangles by the LE-trisection and max-min angle evolution.

**Corollary 1.** If  $t_i$  is a triangle obtained by the LE-trisection of  $t$  and  $\theta$  is an interior angle of  $t_i$ , then  $\theta \geq \lambda/c_1$ , where  $c_1 = \frac{\pi/3}{\arctan(\sqrt{3}/5)} \approx 3.1403$ .

### 3. Empirical study on the non-degeneracy of the partitions obtained by the LE-trisection

Let us begin by describing a Monte Carlo computational experiment used to visualize the evolution of the shape of the triangles generated by the LE-trisection. We will represent all the triangles in a normalized way, that is having the longest-edge of unit length, so that the longest edge of each triangle has as extreme points  $(0,0)$  and  $(1,0)$ . In addition we will suppose that the opposite vertex of the longest-edge is in the upper half plane and also that the smallest angle will be located at vertex  $(1,0)$ . All these conditions imply that every triangle is represented by a point into the mapping domain comprised by the horizontal segment with extreme points  $(0,0)$  and  $(1/2,0)$ , the vertical line of equation  $x = 1/2$  and the exterior circular arc of equation  $(x - 1)^2 + y^2 = 1$  with  $0 \leq x \leq 1/2$  and  $y \geq 0$ .

We proceed as follows: (1) Select a point within the mapping domain. (2) For this selected triangle, the LE-trisection is recursively applied. (3) The apex of each triangle so obtained is represented into the mapping domain.

Algorithm 3.1 performs the recursive LE-trisection of a single triangle given by its three internal angles. The algorithm constructs a ternary tree with apex of triangles as nodes. To visualize the generated subtriangles in the geometric diagram, a plotting function is used. We plot the apex of the triangle using post-order, this is, triangles of the bottom level in the tree are plotted first.

As a matter of example, Fig. 8(a) and (b) show the points into the geometric diagram and Fig. 8(c) and (d) the evolution of the maximum and minimum angles obtained by iterative application of the longest-edge bisection. Fig. 9 performs the same calculations for the LE-trisection. In the geometric diagrams, an initial triangle is selected for refinement and is marked by \*. Each subsequent triangle generated is again plotted in the diagram, resulting so a cloud of round points representing different triangle classes.

It should be noted that points as close as desired may be obtained for a sufficiently large number of LE-trisections. This empirical experiment seems to assert the no existence of a global upper bound of the number of non-similar triangles obtained by LE-trisection. This fact is an important difference with the LE-bisection [12,15].

```

Algorithm 3.1. FUNCTION TRISECTION ( $\tau, \sigma, \rho, Level$ )
Input:  $\tau, \sigma, \rho$  % triangle angles in ascendant order
Input:  $Level$  % Tree level of the recursive trisection process
Output:  $\tau$  % Minimum angle of the new generated subtriangle
if  $Level > 0$ 
    then
         $x = \frac{\tan(\tau)}{\tan(\sigma) + \tan(\tau)}$ ;
         $y = \frac{\tan(\tau) \cdot \tan(\sigma)}{\tan(\sigma) + \tan(\tau)}$ ;
         $A = \sqrt{(x - \frac{1}{3})^2 + y^2}$ ;
         $B = \sqrt{(x - \frac{2}{3})^2 + y^2}$ ;
         $C = \sqrt{(x - 1)^2 + y^2}$ ;
         $\beta_1 = \arccos(\frac{B^2 + C^2 - \frac{1}{9}}{2BC})$ ;
         $\beta_2 = \arccos(\frac{A^2 + B^2 - \frac{1}{9}}{2AB})$ ;
         $\beta_3 = \rho - \sigma_1 - \sigma_2$ ;
         $t_1 = \text{TRISECTION}(\sigma_1, \tau, \pi - \sigma_1 - \tau, Level - 1)$ ;
         $t_2 = \text{TRISECTION}(\sigma_1 + \tau, \sigma_2, \pi - \sigma_1 - \tau - \sigma_2, Level - 1)$ ;
         $t_3 = \text{TRISECTION}(\sigma_1 + \tau + \sigma_2, \sigma_3, \sigma, Level - 1)$ ;
        PLOT TRIANGLE ( $\tau, \sigma, \rho$ ) in the Geometric Diagram
        return  $t_1$ ;
    else
        PLOT TRIANGLE ( $\tau, \sigma, \rho$ ) in the Geometric Diagram
        return  $\tau$ ;

```

Finally, in order to visually illustrate the non-degeneracy property of the LE-trisection Fig. 10 show for each point of the geometric diagram the factor of degeneracy, that means the (color) value of the quotient  $\frac{\tau_0}{\tau_n}$ , being  $\tau_0$  the minimum initial angle and  $\tau_n$  the minimum angle after  $n$  level of depth into the ternary tree. In the diagram of Fig. 10 we have implemented

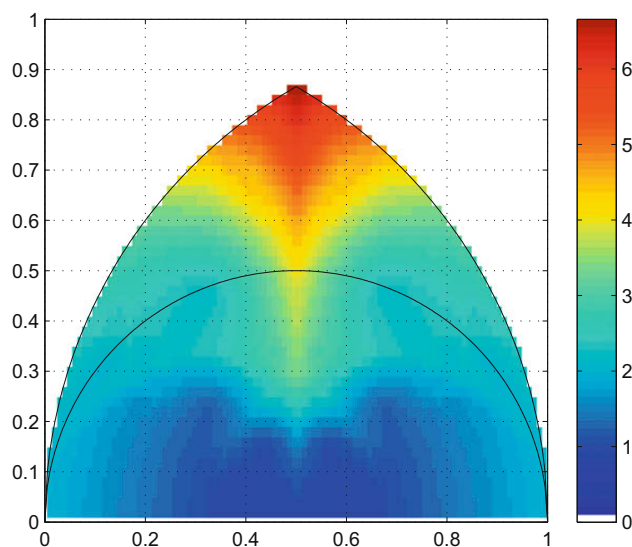


Fig. 10. Values of the quotient  $\frac{\tau_0}{\tau_n}$  for each initial triangle apex.

a ten-level tree, which means that for any initial triangle has been obtained in the bottom level of the tree  $3^{10} = 59049$  triangles. It should be noted that the highest value for the factor corresponds to the equilateral triangles as initial triangle, and its value is  $\sim 6.7052025350$ .

#### 4. Final remarks

Here the non-degeneracy property of the triangular partitions obtained by LE-trisection of triangles has been proved. It has been shown that if  $\tau_1$  is any interior angle of the three triangles obtained by the LE-trisection of an initial triangle  $t_0$  with smallest interior angle  $\tau > 0$ , then  $\tau_1 \geq \tau/3.1403$ , with equality only for the case of an equilateral initial triangle. In addition, experimental evidence of the bound  $\tau_n \geq \tau/6.7052025350$  is given, where  $\tau_n$  is the minimum interior angle after  $n$  iterative trisections. The reduction factor in the minimum angle, 6.7052025350 is attained again in the case of the equilateral initial triangle.

However, some open questions arise here. For example, the study of the number of similarly distinct triangles generated by LE-trisection, the geometry of the points appearing into the geometric diagram by the LE-trisection which will be tackled in forthcoming papers.

#### Acknowledgements

This work has been supported in part by CYCIT Projects numbers MTM2005-08441-C02-02 and MTM2008-05866-C03-02/MTM from Ministerio de Educación y Ciencia of Spain. We wish to thank Javier Miranda, for the implementation of Algorithm 3.1 in ADA [9], and also to the anonymous referees for their helpful comments which improved the presentation of the original version of this paper.

#### References

- [1] A. Adler, On the bisection method for triangles, *Math. Comp.* 40 (162) (1983) 571–574.
- [2] R.E. Bank, PLTMG: A software package for solving elliptic partial differential equations, Users guide 6.0., SIAM, Philadelphia, Penn, 1990.
- [3] J.-H. Choi, K.-R. Byun, H.-J. Hwang, Quality-improved local refinement of tetrahedral mesh based on element-wise refinement switching, *J. Comput. Phys.* 192 (1) (2003) 312–324.
- [4] E.A. Jonckheere, C.K. Chu, Bounded flatness in Q-triangulated regular N-simplexes, *Appl. Math. Comp.* 88 (2–3) (1997) 177–198.
- [5] M.T. Jones, P.E. Plassmann, Computational results for parallel unstructured mesh computations, *Comp. Syst. Eng.* 5 (4–6) (1994) 297–309.
- [6] M.T. Jones, P.E. Plassmann, Adaptive refinement of unstructured finite-element meshes, *Finite Elem. Anal. Design* 25 (1–2) (1997) 41–60.
- [7] K. Kashiwama, T. Okada, Automatic mesh generation method for shallow water flow analysis, *Int. J. Num. Meth. Fluids.* 15 (1992) 1037–1057.
- [8] S. Korotov, M. Krizek, A. Kropac, Strong regularity of a family of face-to-face partitions generated by the longest-edge bisection algorithm, *Comp. Math. Math. Phys.* 48 (9) (2008) 1687–1698.
- [9] J. Miranda, A detailed description of the GNU Ada run time, University of Las Palmas de Gran Canaria, Canary Islands, Spain. Available on-line at <<http://www.iuma.ulpgc.es/users/jmiranda/gnat-rtts>>.
- [10] A. Plaza, G.F. Carey, Local refinement of simplicial grids based on the skeleton, *App. Num. Math.* 32 (2) (2000) 195–218.
- [11] A. Plaza, J.P. Suárez, M.A. Padrón, Non-degeneracy study of the 8-tetrahedra longest-edge partition, *App. Num. Math.* 55 (4) (2005) 458–472.
- [12] A. Plaza, J.P. Suárez, M.A. Padrón, S. Falcón, D. Amieiro, Mesh quality improvement and other properties in the four-triangles longest-edge partition, *Comput. Aided Geomet. Des.* 21 (4) (2004) 353–369.
- [13] M.C. Rivara, Mesh refinement processes based on the generalized bisection of simplices, *SIAM J. Num. Anal.* 21 (1984) 604–613.
- [14] M.C. Rivara, Algorithms for refining triangular grids suitable for adaptive and multigrid techniques, *Int. J. Num. Meth. Eng.* 2 (1984) 745–756.
- [15] I.G. Rosenberg, F. Stenger, A lower bound on the angles of triangles constructed by bisecting the longest-side, *Math. Comp.* 29 (130) (1975) 390–395.
- [16] J.P. Suárez, A. Plaza, G.F. Carey, Propagation of longest-edge mesh patterns in local adaptive refinement, *Commun. Numer. Meth. Engng.* 24 (7) (2008) 543–553.
- [17] M. Stynes, On faster convergence of the bisection method for certain triangles, *Math. Comp.* 33 (146) (1979) 717–721.
- [18] M. Stynes, On faster convergence of the bisection method for all triangles, *Math. Comp.* 35 (152) (1980) 1195–1201.
- [19] O.C. Zienkiewicz, J.Z. Zhu, Adaptivity and mesh generation, *Int. J. Num. Meth. Eng.* 32 (4) (1991) 783–810.